Ground-state magnetization of ^{209}Bi in a dynamic-correlation model

M. Tomaselli,[1] S. M. Schneider,[2] E. Kankeleit,[1] and T. Kühl[3]
[1]*Institut für Kernphysik, Technische Hochschule Darmstadt, Schlossgartenstrasse 9, D-64289 Darmstadt, Germany*
[2]*Institut für Theoretische Physik, Johann Wolfgang Goethe-Universität, Postfach 11 19 32, D-60054 Frankfurt/Main, Germany*
[3]*Gesellschaft für Schwerionenforschung (GSI), Postfach 11 05 52, D-64223 Darmstadt, Germany*
(Received 21 November 1994)

The nuclear magnetization distribution and the magnetic moment of the ground state of ^{209}Bi are calculated within a dynamic-correlation model. The obtained ground-state magnetization reproduces successfully the hyperfine structure splitting (HFS) of mesonic and electronic ^{209}Bi. The evaluated nuclear radius and the electric charge distribution are also in very good agreement with experimental data. The dynamic model is based on the introduction of configuration mixing wave functions (CMWF), generated by breaking the particle-hole symmetry of the ^{208}Pb closed-shell core via the two-body interaction. The 2-particle–1-hole states in this calculation are restricted to a $2\hbar\omega$ configuration space in the protons and in the neutrons. The particle-hole excitations, introduced by this nonperturbative approximation are of collective character and therefore can also be associated with the creation of virtual bosons in the dynamic nuclear structure calculation. In the framework of this dynamic nuclear model it is possible to set a realistic limit for the nuclear contributions for calculations of the $^{209}Bi^{82+}$ hyperfine structure splitting, and therefore to allow, for the first time, a test of QED corrections in the strong magnetic field of high-Z atoms.

PACS number(s): 21.10.Ky, 21.60.−n, 27.80.+w, 31.30.Gs

I. INTRODUCTION

The shell model prediction for the magnetic moment of the ground state of the ^{209}Bi nucleus deviates by nearly a factor 2 from the experimental value.

Perturbation calculations which introduce core-polarization effects via selected particle-hole excitations [1] have improved the value of the calculated magnetic moments. The core-polarization model was extended in Ref. [2] to include in the calculation the effects of the nuclear medium. Within this approximation, comparison of the theoretical and measured values reveals a small discrepancy. This leads to the concept of a "quenching" of the gyromagnetic factors, associated with the appearance of the meson degrees of freedom in the nuclear structure calculation [3].

The nonperturbative theory of Ref. [4], provides a consistent treatment the core-polarizations and the "quenching factors" in a dynamic approximation. In various numerical applications [5,6] good agreement between the calculated and the measured magnetic properties of nuclei has been achieved. The theoretical calculations have been performed within the framework of exact factorization methods which simplify the computation of the matrix elements of the model operators in the dynamic-correlated basis.

In this paper we apply the dynamic-correlation model of Ref. [4] to the calculation of the nuclear ground-state properties of ^{209}Bi.

The correlated dynamics generated in this case by the residual interaction between the valence proton and the particles of the model vacuum, lead to configuration mixing wave functions (CMWF). The CMWF are obtained by allowing the valence proton in the $1h_{9/2}$ state to excite the core via proton and neutron particle-hole excitation ($2\hbar\omega$). The structure of the closed-shell vacuum states (particle-hole coupled to $J \neq 0$) modifies the valence-particle configuration space, generating the coupling of the valence-particle states with (a) closed shell polarizations of normal parity, (b) closed shell polarizations of non-normal parity. These states have the same quantum numbers as the low-energy mesons ($\omega, \rho, \ldots$) and are characterized, in this nonperturbative approximation, by many particle-hole pairs mixed via the two-body interaction to the valence states.

As we will discuss in Sec. IV, the amplitudes of these modes, calculated with a specific choice of the parameters of the theory (single-particle energies and two-body potential) as in Refs. [19–21], contribute coherently to the formation of the magnetic distribution of ^{209}Bi. If we will associate this coherent effect to the degree of collectivity of the model, we may state that these non-normal parity polarizations are in the present calculation very well represented as collective states.

This model is therefore able to include in the calculation of the magnetic moments of nuclei the core polarization and the quenching (meson) effects within the same formalism, because the nonlinear terms introduced within this model generate a two-body current which describes the exchange of virtual mesons between two nucleons in a nuclear system. The nonlinear terms modify the structure of the single-particle operators postulated at the beginning of the particle-hole iteration process.

The Green functions of the model are defined by the amplitudes of the valence-core wave functions (CMWF) which are calculated by the equation-of-motion method

as described in Ref. [4]. A direct comparison of this nonlinear approximation with mean-field models is therefore feasible.

The calculated wave functions are used to describe the magnetic and the electric properties of the ground state of ^{209}Bi. The rms radius and the nuclear charge distribution have been additionally calculated, and the agreement with the already calculated nuclear charge distributions in the ^{208}Pb region as well as the charge radii [7] is satisfactory.

The realistic nuclear magnetic distribution, as calculated in this model, allows us to evaluate the Bohr-Weisskopf contribution to the hyperfine structure splitting of a hydrogenlike ion and to compare, therefore, the theoretical result with the experimentally measured value [8]. As we will discuss in Sec. IV, an overall, almost perfect agreement with the experimental values for the nuclear ground-state properties has been obtained.

The calculation can be extended to other nuclei with one particle or one hole in the closed-shell nucleus. The results of Ref. [5] for the thallium 203 and 205 isotopes have been successfully reanalyzed in Ref. [9] where the dependence of the hyperfine structure on the magnetic moment distributions has been discussed.

In the next sections we will discuss the model and then use it to calculate the HFS splitting.

II. MIXING OF THE DYNAMIC-CORRELATION CMWF

In this paper the electromagnetic properties of ground and excited states of nuclei with one particle outside the closed shells are described within an extended dynamic correlation model. The residual interaction between the valence and the core particles causes the deformation of the nuclear core.

The effect of the extended nuclear core is included in the present calculation defining model wave functions, the CMWF [4]. In this paper the hierarchy of the configuration-mixing wave functions is linearized so to include in the calculation only the CMWF of the first type which are characterized by the $2p$-$1h$ states resulting from the vector coupling of the valence particle with the $1p$-$1h$ core excitations. The higher order CMWF ($3p$-$2h$) have been linearized to generate the dynamic eigenvalue equations of the model. According to this linearization approximation, the ground-state wave function $\{\phi_{jm}\}$ of the $|A+1\rangle$ nucleus is defined as

$$|\phi_{jm}\rangle = \left[\chi^0_{\alpha_0 j} a^\dagger_{jm} + \sum_{j_1 j_2 j_3 J_1} \chi^1_{j_1 j_2 j_3 J_1 j} N^1_{j_1 j_2 j_3 J_1 j} \times A^\dagger_1(j_1(j_2 j_3)J_1; jm)\right]|0\rangle$$
$$= \left[\chi^0_{\alpha_0 j} a^\dagger_{jm} + \sum_{\alpha_1 J_1} \chi^1_{\alpha_1 J_1 j} N^1_{\alpha_1 J_1 j} A^\dagger_1(\alpha_1 J_1; jm)\right]|0\rangle \ , \tag{2.1}$$

where the operator $a^\dagger_{jm}$ creates a single valence proton with quantum numbers $\{j, m\}$ and where the operator

$$A^\dagger_1(\alpha_1 J_1; jm) = A^\dagger_1(j_1(j_2 j_3)J_1; jm) = \sum_{m's} [a^\dagger_{j_1} \otimes (a^\dagger_{j_2} \otimes a_{j_3})^{J_1}]^j_m |0\rangle$$

creates the $2p$-$1h$ states, obtained, as indicated by the notation $[a^\dagger_{j_1} \otimes (a^\dagger_{j_2} \otimes a_{j_3})^{J_1}]^j_m$, by coupling the valence proton with quantum number $\{j_1\}$ to the particle-hole pair with quantum numbers $\{j_2\}$ and $\{j_3^{-1}\}$, respectively. The symbol $|0\rangle$ defines the model vacuum. The $\{N\}$ specifies the norm, and the $\{\chi\}$'s denote the mode amplitudes. The superscript $\{1\}$ in the N's and χ's as well as the subscript $\{1\}$ of the A's, characterize the excitation of one particle-hole pair.

If the quantum numbers of the valence particle $\{j_1\}$ are not equal to the quantum numbers of the core particle $\{j_2\}$, the set of states [Eq. (2.1)] is orthonormal, otherwise not. In the latter case the states are normalized via the orthogonalization procedure of Schmidt [10], which consists in evaluating the overlap integrals between the two nonorthogonal $A^\dagger_1[j_1(j_1 j_3)J_1; j]$ and $A^\dagger_1[j_1(j_1 j_3)J'_1; j]$ states. With these integrals we define the orthogonal states as linear combination of the form

$$\phi^2_{jm}(\alpha_1 J_1)|0\rangle = \frac{1}{N}[\phi^1_{jm}(\alpha_1 J_1) - \langle A_1(\alpha_1 J_1)|A^\dagger_1(\alpha_1 J'_1)\rangle \times \phi^1_{jm}(\alpha_1 J'_1)]|0\rangle \ .$$

The amplitudes of the different modes ($\chi^0_{\alpha_0 j}$ and $\chi^1_{\alpha_1 J_1 j}$) in the linearized Eqs. (2.2) and (2.3) are calculated in the dynamic approximation of Ref. [4]. This approximation consists in evaluating the chain of commutators

$$[H, a^\dagger_{jm}] = [H, A^\dagger_0(\alpha_0; j)] = \sum_{\alpha'_0} \epsilon_j A^\dagger_0(\alpha'_0; j) + \sum_{\alpha_1 J_1} \langle A_0(\alpha_0; j)||V||A^\dagger_1(\alpha_1 J_1; j)\rangle A^\dagger_1(\alpha_1 J_1; j) \ , \tag{2.2}$$

$$[H, A^\dagger_1(\alpha_1 J_1; j)] = \sum_{\alpha'_0} \langle A_1(\alpha_1 J_1; j)||V||A^\dagger_0(\alpha'_0; j)\rangle A^\dagger_0(\alpha'_0; j) + \sum_{\alpha'_1 J'_1} \langle A_1(\alpha_1 J_1; j)||H||A^\dagger_1(\alpha'_1 J'_1; j)\rangle A^\dagger_1(\alpha'_1 J'_1; j)$$
$$+ \sum_{\alpha''_2 J''_1 J''_2} \langle A_1(\alpha J_1; j)||V||A^\dagger_2(\alpha''_2 J''_1 J''_2; j)\rangle A^\dagger_2(\alpha''_2 J''_1 J''_2; j) \tag{2.3}$$

and linearizing the $A_2^\dagger(\alpha_2'' J_1'' J_2''; j)$ terms in order to obtain, in the first-order linearization approximation, the eigenvalue equation for the $\{\chi\}$ amplitudes

$$\chi_j^0 = \langle \Phi_0(A) | a_{jm} | \Phi_p(A+1) \rangle$$

$$\chi^1_{j_1(j_2 j_3) J_{1j}} = \langle \Phi_0(A) | A_1(j_1(j_2 j_3) J_1) | \Phi^1_{2p1h}(A+1) \rangle \ .$$

In (2.2) and (2.3) the nuclear Hamiltonian is

$$H = \sum_\alpha \epsilon_\alpha a_\alpha^\dagger a_\alpha + \frac{1}{2} \sum_{\alpha\beta\gamma\delta} V_{\alpha\beta\gamma\delta} a_\alpha^\dagger a_\beta^\dagger a_\delta a_\gamma = H_0 + V \ ,$$

where $V_{\alpha\beta\gamma\delta}$ are the matrix elements of the two-body potential V

$$V_{\alpha\beta\gamma\delta} = (\alpha\beta | V | \gamma\delta) \ ,$$

and ϵ_α are the single-particle energies. These can be either calculated in the HF approximation or, as assumed in this work, taken from the low-lying spectrum of neighboring closed-shell nuclei. The single-particle wave functions used to calculate the matrix elements of the two-body potentials have been approximated with harmonic oscillator wave functions and the two-body potential have been assumed to have the form

$$V = e^{-(\frac{r}{b})^2} \sum_{S,T} V_{ST} P_{ST}$$

where P_{ST} are the projection operators of the two-body states with quantum numbers S and T and where the parameters V_{ST} are discussed in the Sec. IV.

To calculate the matrix elements of the two-body interaction in Eqs. (2.2) and (2.3) we use the recoupling algebra of Ref. [11]. We obtain

$$\langle A_0(\alpha_0; j) || V || A_1^\dagger(\alpha_1 J_1; j) \rangle = \sum_{J_i} (-1)^{j+j_2+J_i+J_1} (2J_i+1) \sqrt{\frac{2J_1+1}{2j+1}} \begin{Bmatrix} j & j_3 & J_i \\ j_2 & j_1 & J_1 \end{Bmatrix} \langle j j_3 | V | j_1 j_2 \rangle^a_{J_i} \tag{2.4}$$

$$\begin{aligned}
&\langle A_1(\alpha_1 J_1; j) || V || A_1^\dagger(\alpha_1' J_1'; j) \rangle \\
&= \sum_{J_i} (-1)^{J_i+j_3+J_2'} (2J_i+1) \begin{Bmatrix} j_3 & j_2' & J_i \\ j_3' & j_2 & J_1 \end{Bmatrix} \langle j_3 j_2' | V | j_2 j_3' \rangle^a_{J_i} \delta_{J_1 J_1'} \\
&+ \sum_{J_i} (-1)^{1+j_2'+j_2+J_1+J_1'} (2J_i+1) \sqrt{(2J_1+1)(2J_1'+1)} \begin{Bmatrix} j_2' & j_3 & J_1' \\ j & j_1' & J_i \end{Bmatrix} \begin{Bmatrix} j_2 & j_3 & J_1 \\ j & j_1 & J_i \end{Bmatrix} \langle j_1' j_2' | V | j_1 j_2 \rangle^a_{J_i} \\
&+ \sum_{J_i} (-1)^{j_1+j_3+J_i} (2J_i+1) \begin{Bmatrix} j_3 & j_1 & J_i \\ j_3' & j_2 & J_1 \end{Bmatrix} \langle j_3 j_1 | V | j_2 j_3' \rangle^a_{J_i} \delta_{J_1 J_1'} \\
&+ \sum_{J_r J_i} (-1)^{j_1+j_2+j_3'+J_1+J_1'+j} (2J_r+1)(2J_i+1) \sqrt{(2J_1+1)(2J_1'+1)} \begin{Bmatrix} J_1 & j_3 & j_2 \\ j_3' & J_1' & J_r \end{Bmatrix} \\
&\times \begin{Bmatrix} j_3 & j_1' & J_i \\ j_1 & j_3' & J_r \end{Bmatrix} \begin{Bmatrix} J_1 & j_1 & j \\ j_1' & J_1' & J_r \end{Bmatrix} \langle j_3 j_1' | V | j_1 j_3' \rangle^a_{J_i} \\
&+ \sum_{J_r J_i} (-1)^{j_1+j_2+j_3'+J_1+J_1'+j} (2J_r+1)(2J_i+1) \sqrt{(2J_1+1)(2J_1'+1)} \begin{Bmatrix} J_1 & j_3 & j_2 \\ j_3' & J_1' & J_r \end{Bmatrix} \\
&\times \begin{Bmatrix} j_3 & j_2 & J_i \\ j_1 & j_3' & J_r \end{Bmatrix} \begin{Bmatrix} J_1 & j_1 & j \\ j_2 & J_1' & J_r \end{Bmatrix} \langle j_3 j_1' | V | j_1 j_3' \rangle^a_{J_i} \ .
\end{aligned} \tag{2.5}$$

In Eqs. (2.4) and (2.5) $\begin{Bmatrix} abc \\ def \end{Bmatrix}$ denotes the 6-J symbols as defined in Ref. [11] and the $\langle j_a j_b | V | j_c j_d \rangle^a_{J_i}$ are the antisymmetrized two-body matrix elements:

$$\langle j_a j_b | V | j_c j_d \rangle^a_{J_i} = \langle [j_a j_b]^{J_i} | V | [j_c j_d]^{J_i} - [j_d j_c]^{J_i} \rangle \ .$$

Taking the expectation value of Eqs. (2.2) and (2.3) between the vacuum and the state $[|\phi_{jm}(1p+2p1h)\rangle]^\dagger$ we obtain the eigenvalue equation that defines the amplitudes $\chi^0_{\alpha_0 j}$ and $\chi^1_{\alpha_1 J_{1j}}$ of the nuclear modes. We obtain

$$\sum_{\substack{j_1 j_2 j_3 \\ j_1' j_2' j_3'}} \begin{vmatrix} E+\epsilon_j & V_{jj_3' j_1' j_2'} \\ V_{j_1 j_2 j j_3} & E+\epsilon_{j_1}+\epsilon_{j_2}-\epsilon_{j_3}+V_{j_1 j_2 j_3 j_1' j_2' j_3'} \end{vmatrix} \begin{vmatrix} \chi^0_{\alpha_0 j} \\ \chi^1_{\alpha_1 J_{1j}} \end{vmatrix} = 0 \ . \tag{2.6}$$

Equation (2.6) is suitable to describe, with $V_{jj_3j_1j_2} = V_{j_1'j_2'jj_3'} = 0$, also the excited septuplet states of ^{209}Bi as well as ground and excited states of the odd $A+1$ nuclei, the generalization of Eq. (2.6) to the isospin quantum numbers that one needs to describe the spectrum of light-medium mass nuclei as been defined in Ref. [6].

For the ground state of ^{209}Bi Eq. (2.6), with $j = 9/2$, is highly nonlinear including explicitly in the calculation (in a nonperturbative approximation) the $2p$-$1h$ model spaces. In the present calculation the sum over the $2p$-$1h$ states is truncated according to an energy cut off. Only states with Hartree-Fock energies $\epsilon_p + \epsilon_{p'} - \epsilon_h \leq 10$ MeV have been included in the numerical analysis. The cut-off parameter has been introduced to limit the dimension of the eigenvalue matrix (2.6) which, in the present calculation, has the dimension 450×450.

Diagonalizing Eq. (2.6) we calculate the dynamic amplitudes of the ground-state modes. These amplitudes are taken to evaluate the reduced matrix elements of the operators O^λ that characterize the electromagnetic moment of order λ.

With some recoupling operations we obtain for the reduced transition-matrix elements:

$$\langle A_0(\alpha_0 j)||O^\lambda||A_0(a_0' j')\rangle = \chi^0_{\alpha_0 j}\chi^{0'}_{\alpha_0' j'}(j||O^\lambda||j') \ , \tag{2.7}$$

$$\langle A_0(\alpha_0 j)||O^\lambda||A_1(\alpha_1' J_1'; j')\rangle = \chi^0_{\alpha_0 j}\chi^{1'}_{\alpha_1' J_1 j'}\Bigg[(-1)^{j_2'+j_3'}\sqrt{2j_1'+1/2\lambda+1}(j_3'||O^\lambda||j_2')\delta_{\lambda J_1'}\delta_{j_1' j} + (-1)^{j_3'+j_1'}\cdot\sqrt{(2j_1'+1)(2J_1'+1)}\begin{Bmatrix} j & j_3' & J_1' \\ j_1' & j' & \lambda \end{Bmatrix}(j_3'||O^\lambda||j_1')\delta_{j_2' j}\Bigg] \ , \tag{2.8}$$

$$\begin{aligned}\langle A_1(\alpha_1 J_1; j)||O^\lambda||A_1^\dagger(\alpha_1' J_1'; j')\rangle &= \chi^1_{\alpha_1 J_1 j}\chi^{1'}_{\alpha_1' J_1' j'} \\ &\times\sqrt{(2j+1)(2j'+1)(2J_1+1)(2J_1'+1)}\Bigg[(-1)^{j_3'+J_1+J_1'+j}\begin{Bmatrix} j_3' & j_3 & \lambda \\ j_1' & J_1 & j \\ J_1' & j_2 & j' \end{Bmatrix}(j_3'||O^\lambda||j_3) \\ &+(-1)^{j_2+j_3+j_1'+j}\begin{Bmatrix} J_1' & j_3' & j_2 \\ j_3 & J_1 & \lambda \end{Bmatrix}\begin{Bmatrix} J_1' & j' & j_1' \\ j & J_1 & \lambda \end{Bmatrix}(j_3'||O^\lambda||j_3) \\ &+(-1)^{j_1'+j_2+j_3+j'+J_1+J_1'}\begin{Bmatrix} j_2' & J_1' & j_3 \\ J_1 & j_2 & \lambda \end{Bmatrix}\begin{Bmatrix} J_1' & j' & j_1' \\ j & J_1 & \lambda \end{Bmatrix}(j_2||O^\lambda||j_2') \\ &+\frac{(-1)^{J_1+j_1'+j+\lambda}}{\sqrt{(2J_1+1)(2J_1'+1)}}\begin{Bmatrix} j' & j_1' & J_1 \\ j_1 & j & \lambda \end{Bmatrix}(j_1||O^\lambda||j_1') \\ &+(-1)^{j_2'+j+J_1+\lambda}\begin{Bmatrix} j_2' & j_3 & J_1' \\ j_2 & j & J_1 \end{Bmatrix}\begin{Bmatrix} J_1 & j & j_1' \\ \lambda & j_2' & j' \end{Bmatrix}(j_1||O^\lambda||j_2') \\ &+(-1)^{j_1'+j+J_1'+\lambda}\begin{Bmatrix} j_2 & j_3 & J_1 \\ j_1 & j & J_1' \end{Bmatrix}\begin{Bmatrix} j_2 & \lambda & j_1' \\ j' & j_1 & j \end{Bmatrix}(j_2||O^\lambda||j_1')\Bigg] \ . \end{aligned} \tag{2.9}$$

In Eqs. (2.7), (2.8), and (2.9) the operator O^λ is representing successively the magnetic moment, the quadrupole moment, the hyperfine structure splitting, and the magnetic- and electric-distribution operators. In Eq. (2.9)

$$\begin{Bmatrix} a & b & c \\ d & e & f \\ g & h & i \end{Bmatrix}$$

is the $9J$ symbol and the reduced matrix elements are defined according to Ref. [11].

If the operator O^λ is associated with the magnetic-moment operator $\sum_{\alpha\beta}(\alpha|g_l l_z + g_s s_z + \beta)a_\alpha^\dagger a_\beta$, the reduced matrix element on the right-hand side of Eq. (2.7) is equivalent to the Schmidt value when the single-particle amplitudes $\chi^0_{\alpha_0 j}$ and $\chi^0_{\alpha_0' j'}$ are neglected.

Unlike calculations done in the first-order approximation, the right side of Eq. (2.8) takes properly into account the antisymmetric terms resulting by interchanging valence and core particles. The terms of Eq. (2.9) have been included exactly in the present calculations. They contribute coherently to the formation of the magnetic distribution in nuclei. These terms are, in a perturbative approximation, approximated by the second-order contributions of the theory, if we neglect the Pauli-antisymmetrization principle. This comparison between our calculation and the perturbative calculation is only to be considered formal, because due to our diagonal-

ization method and to the large number of components introduced, the CMWF of the model may be associated with the collective modes of the nucleus.

III. INTERACTION WITH THE ATOMIC MAGNETIC FIELD

Exotic atoms, i.e., atoms with configurations deviating strongly from conditions typically realized in nature, offer fascinating possibilities for testing nuclear models. Such exotic atoms exhibit the interplay of nuclear and atomic quantities. They permit one to test specific parts of the electromagnetic interaction by selectively changing or observing the effect of just a single parameter much as precise studies have been made in the past using muonic atoms.

It is now possible to produce a wide variety of exotic atoms from energetic heavy-ion collisions. For example, at GSI [8] in Darmstadt hydrogenlike high-Z atoms such as $^{209}Bi^{82+}$ have recently become available for experiments. They are produced from heavy ions accelerated to several hundred MeV/u at the SIS accelerator. Because they are then stored and cooled in the ESR storage ring, they can be studied without the usual constraints of unsatisfactory accelerator-beam quality and short observation time. Where previously only the ground-state hyperfine-structure (HFS) splitting in muonic ^{209}Bi [15,16] could be studied, it is now possible to investigate the corresponding electronic effects in the hydrogenlike Bi ion.

Because the HFS splitting is proportional to Z^3, the wavelength of the $M1$ transition between the ground-state components of hydrogenlike ions with high Z is in the optical regime. (This is dramatically different from the case of hydrogen where the HFS splitting is in the microwave regime—the 21-cm radiation.) As a result it was possible to measure the ground-state HFS splitting of hydrogenlike Bi^{82+} by laser-induced fluorescence spectroscopy [8]. The experiment yielded a ground-state energy splitting of $\Delta E^{\rm ex} = 5.0841(8)$ eV and achieved a relative accuracy of $\simeq 10^{-4}$. This high accuracy has made possible the first test of QED in the strong magnetic field of the highly charged heavy ion.

For the case of a heavy ion like Bi^{82+}, the large nucleus will have three significant effects on the HFS splitting: (a) There will be an effect due to the extended nuclear charge distribution—Breit-Rosenthal effect; (b) an effect due to the finite nuclear magnetization distribution—Bohr-Weisskopf effect; and (c) radiative corrections of order α—QED effects. The energy splitting also depends strongly on the rms radius of the nuclear charge distribution, but different charge parametrizations give similar results.

The energy shift due to the vacuum-polarization part of the radiative corrections has been calculated recently to be $\Delta E^{\rm VP} = -0.035$ eV [17]. This means that for high-Z atoms, QED and nuclear-magnetization corrections are of the same order of magnitude. Therefore, the feasibility of testing the QED corrections depends strongly on the accuracy of the model used to evaluate the effects of nuclear magnetization. Since the QED corrections are continuous functions of A and Z, while the magnetic distributions in neighboring isotopes can differ significantly, it may be possible to distinguish the nuclear contributions from the QED corrections by measurements on different isotopes.

In this paper the essential nuclear parameters are calculated using the dynamic-correlation model. The electron (μ meson) is described as a Dirac particle moving in the Coulomb potential generated by a charge distribution of a Fermi type. The magnetic interaction of the electron (μ meson) with charge of the nucleus is given by

$$V_{(e_\mu)-N} = e\int d^3\vec{r}_{(e_\mu)}\psi^*_{(e_\mu)}\left(\vec{r}_{(e_\mu)}\right)\vec{\alpha} \cdot\vec{A}_{(e_\mu)}\left(\vec{r}_{(e_\mu)}\right)\psi_{(e_\mu)}\left(\vec{r}_{(e_\mu)}\right) ,$$

where

$$\vec{A}\left(\mathbf{r}_{(e_\mu)}\right) = -\int d^3\vec{r}_n\vec{m}(\vec{r}_n)\times\nabla_{(e_\mu)}\frac{1}{|\vec{r}_{(e_\mu)}-\vec{r}_n|}$$

with

$$\vec{m}(\vec{r}_n) = \mu_0\sum_i(g^i_l\vec{l}_i + g^i_s\vec{s}_i)\delta(\vec{r}_n-\vec{r}_i) .$$

From these expressions, expanding $\vec{A}(\mathbf{x})$ in multipole and using some recoupling, we obtain, according to Ref. [18]

$$\Delta E = C(A_L + A_S) \tag{3.1}$$

with

$$C = \frac{F(F+1)-I(I+1)-j(j+1)}{2Ij}\Bigg|_{F_1}^{F_2} ,$$

where F designates the total angular momentum quantum number of the electron (muon)-nucleus system. I is the angular momentum quantum number of the nucleus, and j the angular momentum quantum number of the electron (muon), so that $|F_1| \le F \le F_2$. In the case of $^{209}Bi^{82+}$ the total angular momentum quantum number for the ground state is $F_1 = |I-j| = 9/2-1/2 = 4$, and for the first excited HFS state $F_2 = I+j = 9/2+1/2 = 5$. This leads to the value

$$\Delta E = (C_1 - C_2)(A_L + A_S) = (20/9)(A_L + A_S) .$$

The A_L and A_S are the orbital-angular-momentum part and the spin-angular-momentum part, respectively. For the ground state (2.1) they are given by

$$A_L = \frac{4}{3}e\mu_0\langle\phi_{jm}|\sum_{\alpha\beta}(\alpha|O_L|\beta)a^\dagger_\alpha a_\beta|\phi_{jm}\rangle \tag{3.2}$$

and

$$A_S = \frac{4}{3}e\mu_0\langle\phi_{jm}|\sum_{\alpha\beta}(\alpha|O_S|\beta)a^\dagger_\alpha a_\beta|\phi_{jm}\rangle , \tag{3.3}$$

where

$$O_L = g_l l_z \left[\int_R^\infty f(r)g(r)dr + \int_0^R \left(\frac{r}{R}\right)^3 f(r)g(r)dr \right] \tag{3.4}$$

and

$$O_S = g_s s_z \int_R^\infty f(r)g(r)dr - \sqrt{\frac{\pi}{2}}[Y_2 \otimes \sigma]^1 \int_0^R \left(\frac{r}{R}\right)^3 f(r)g(r)dr \ . \tag{3.5}$$

In Eqs. (3.3), (3.4), and (3.5) μ_0 is the nuclear magneton, g_l and g_s are the orbital and spin g factors, the notation $[Y_2 \otimes \sigma]^1$ means the coupling of Y_2 with the nucleon spin operator σ to a spherical tensor of rank one, f and g are the Dirac spinors, and $\{\phi_{jm}\}$ is the ground state wave function [see Eq. (2.1)]. The results of the calculation of the hyperfine structure splitting are presented in Table I and will be discussed in the following section.

To solve the Dirac equation we have approximated the nuclear density distribution with a two-parameter Fermi distribution as in de Vries *et al.* [24].

Up to now, only the vacuum-polarization part of the radiative corrections to order α have been calculated [18]. Since this effect yields

$$\Delta E^{VP} = +0.035 \text{ eV or } \Delta\lambda = -1.6 \text{ nm} \ ,$$

the importance of the determination of the self-energy part of the radiative corrections in order to explain theoretically the experimental value is evident.

TABLE I. The square of the amplitude of the single particle and of the terms corresponding to the first-order contributions calculated for the ground state of ^{209}Bi from the diagonalization of the eigenvalue Eq. (2.6).

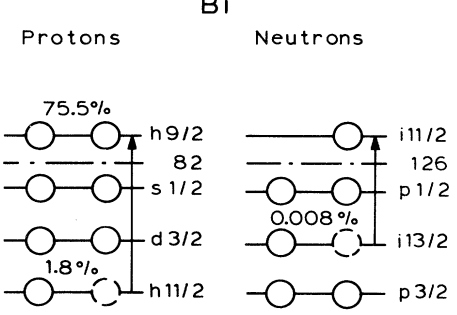

IV. RESULTS AND DISCUSSION

To calculate the electromagnetic properties of the ground state of ^{209}Bi, we have to make some assumption about the input parameters of the model: i.e., single-particle wave functions, single-particle energy, and two-body potential. The single-particle wave functions have been approximated by harmonic oscillation wave functions with the following range:

Proton hole:

$$2p_{3/2}, 1f_{5/2}, 2p_{1/2}, 1g_{9/2}, 2d_{5/2}, 1g_{7/2}, 3s_{1/2}, 2d_{3/2}, 1h_{11/2} \ .$$

Proton particle:

$$1h_{9/2}, 2f_{7/2}, 3p_{3/2}, 2f_{7/2}, 3p_{1/2}, 1i_{13/2}, 3d_{5/2}, 2g_{7/2}, 4s_{1/2}, 3d_{3/2}, 2h_{11/2} \ .$$

Neutron hole:

$$3d_{5/2}, 1g_{7/2}, 3s_{1/2}, 2d_{3/2}, 1h_{11/2}, 1h_{9/2}, 2f_{7/2}, 3p_{3/2}, 2f_{5/2}, 3p_{1/2}, 1i_{13/2} \ .$$

Neutron particle:

$$3d_{5/2}, 2g_{7/2}, 4s_{1/2}, 3d_{3/2}, 2h_{11/2}, 1j_{15/2}, 1i_{11/2}, 2g_{9/2} \ .$$

The single-particle energies are those of Kuo [19].

In Eqs. (2.5) two types of two-body matrix elements occur: (1) particle-hole matrix elements $\langle j_3 j_2' | V | j_2 j_3' \rangle^a_{J_i}$, $\langle j_3 j_1 | V | j_2 j_3' \rangle^a_{J_i}$, and $\langle j_3 j_1' | V | j_1 j_3' \rangle^a_{J_i}$; (2) particle-particle matrix elements $\langle j_1' j_2' | V | j_1 j_2 \rangle^a_{J_i}$.

The two-body model potential, used to calculate the particle-hole matrix elements (1), is taken from Ref. [20] (V_{ST} of COP type) while the two-body model potential, used to calculate the particle-particle matrix elements (2), is taken from Ref. [21].

The matrix elements of Eq. (2.4) are of mixed type and are calculated from particle-particle potential. This particle-hole potential has been already successfully applied in the theoretical description of the septuplet states in ^{209}Bi (See Ref. [22]), while the V_{ST} parameters of the particle-particle potential have been derived by fitting

TABLE II. List of the square of the more significant amplitudes calculated diagonalizing Eq. (2.6). The valence proton is coupled to proton particle-hole states. The amplitudes are small, but give a coherent contribution to the magnetic distribution of the ground state of ^{209}Bi.

Proton configurations	Amplitudes (%)
$1h_{9/2}(1i_{13/2}1g^{-1}_{9/2})_{2+}$	0.132
$1h_{9/2}(2f_{7/2}1h^{-1}_{11/2})_{2+}$	0.041
$1h_{9/2}(2h_{9/2}2p^{-1}_{3/2})_{3+}$	0.176
$1h_{9/2}(1i_{13/2}1g^{-1}_{9/2})_{3+}$	0.271
$1h_{9/2}(1h_{9/2}2p^{-1}_{1/2})_{4+}$	0.016
$1h_{9/2}(1i_{13/2}1g^{-1}_{9/2})_{4+}$	0.045
$1h_{9/2}(1i_{13/2}2d^{-1}_{5/2})_{4+}$	0.092
$2f_{5/2}(1i_{13/2}2d^{-1}_{5/2})_{4+}$	0.037
$1h_{9/2}(1i_{13/2}2d^{-1}_{3/2})_{5+}$	0.014
$2f_{7/2}(1i_{13/2}2d^{-1}_{3/2})_{5+}$	0.019
$2p_{3/2}(1i_{13/2}2d^{-1}_{5/2})_{5+}$	0.013
$1i_{13/2}(1h_{9/2}1g^{-1}_{7/2})_{2-}$	0.059
$1i_{13/2}(2f_{7/2}3d^{-1}_{3/2})_{2-}$	0.156
$1i_{13/2}(1i_{13/2}1i^{-1}_{11/2})_{2-}$	0.191
$1i_{13/2}(1h_{9/2}2p^{-1}_{3/2})_{3-}$	0.037
$1i_{13/2}(2f_{7/2}2f^{-1}_{3/2})_{3-}$	0.029

the two-body matrix elements calculated with the Bethe-Goldstone formalism as described in Ref. [21]. The depth of the particle-hole potential is chosen to reproduce the energy of the first 3^- state in ^{208}Pb. The particle-particle potential has been adjusted to reproduce the level scheme of ^{210}Bi [21] and to calculate the microscopic composition of the excited septuplet states in ^{209}Bi as preliminarily shown in Ref. [23]. The single particle wave functions are assumed to be harmonic oscillator wave functions with size parameters chosen to reproduce Woods-Saxon wave functions, as proposed in Ref. [20], Table I, Table II.

TABLE III. List of the square of the more significant amplitudes calculated diagonalizing Eq. (2.6). The valence proton is coupled to neutron particle-hole states. The amplitudes are small, but give a coherent contribution to the magnetic distribution of the ground state of ^{209}Bi.

Neutron configurations	Amplitudes (%)
$2f_{7/2}(1i_{11/2}1i^{-1}_{13/2})_{1+}$	0.011
$3p_{3/2}(1j_{15/2}1h^{-1}_{9/2})_{3+}$	0.001
$2f_{5/2}(2g_{7/2}1i^{-1}_{13/2})_{3+}$	0.014
$1h_{9/2}(1j_{15/2}1h^{-1}_{9/2})_{4+}$	0.005
$2f_{5/2}(1j_{15/2}2f^{-1}_{7/2})_{4+}$	0.003
$2f_{5/2}(3d_{5/2}1i^{-1}_{13/2})_{4+}$	0.006
$2p_{1/2}(2g_{9/2}1i^{-1}_{13/2})_{4+}$	0.015
$1i_{13/2}(3d_{3/2}3p^{-1}_{1/2})_{2-}$	0.044
$1i_{13/2}(2g_{9/2}3p^{-1}_{1/2})_{5-}$	0.048
$1i_{13/2}(1i_{11/2}1h^{-1}_{9/2})_{5-}$	0.017
$1i_{13/2}(1j_{15/2}3p^{-1}_{1/2})_{5-}$	0.038
$1i_{13/2}(2g_{9/2}3p^{-1}_{1/2})_{5-}$	0.361
$1i_{11/2}(2g_{9/2}3p^{-1}_{3/2})_{5-}$	0.028

TABLE IV. Calculated rms radius, nuclear magnetic moment, nuclear quadrupole moment, and HFS structure for the muonic and electronic ^{209}Bi ground states compared with the experimental results. Note that in the case of the HFS structure for the $^{209}Bi^+$ ground state, the experimental value has been extracted from the experiment without taking in consideration QED corrections.

		Experimental	Theoretical
rms radius	[24]	5.519(2) fm	5.6 fm
Magnetic moment	[25]	4.1106(2) n.m.	4.11 n.m.
$\mu_l - \mu_s$			4.43−0.32
(Schmidt value)			(2.62 n.m.)
Quadrupol moment	[25]	−0.40	−0.35
ΔE for $s_{1/2}$ muon	[15]	4.44(15) keV	4.45 keV
ΔE for $s_{1/2}$ muon dipole approximation			6.65 keV
ΔE for $s_{1/2}$ electron	[8]	5.0841(8) eV	5.091 eV
ΔE for $s_{1/2}$ electron dipole approximation			5.198 eV

With these parameters, diagonalizing the Eq. (2.6) we obtain the wave functions tabulated in Tables I, II, and III. In Table I we give the larger 1^+ amplitudes calculated within this model. In Table II and Table III we give the other more significant ($2p$-$1h$) amplitudes. Although they are small compared with the 1^+ amplitudes of Table I, they contribute coherently to the magnetic structure of bismuth, as in the case of a magnetic-giant resonance, due to the formation of the collective degrees of freedom.

In Table IV we compare the calculated nuclear magnetic moment, the nuclear quadrupole moment, the nuclear rms radius, and the hyperfine structure splitting for muonic and electric ^{209}Bi with the experimental quantities. The agreement between experiment and theoretical values is remarkably good.

For the magnetic moment we give also the single-particle value and the calculated orbital and spin contributions. The small discrepancy between the computed nuclear radius and the experimentally quoted one is probably due to the $4p$-$3h$ components not included in the calculations (CMWF of the second kind which allow for the formation of low lying $\{0^+\}$ states [4]). On the other hand, the calculated nuclear radius agrees remarkably well with the calculation done within the framework of a relativistic mean-field theory [7]. In order to discuss the influence of the extended nuclear charge magnetization distribution on the hyperfine structure splitting, we have also tabulated the results for the dipole approximation.

The muonic atom and the electronic atom are different in one important respect: in the latter scenario the electronic wave function is almost constant over the full extension of the magnetization distribution but the muonic wave function changes significantly in this region.

In contrast to the situation in the electronic-hydrogenlike ion, in the muonic atom the QED contributions to the HFS are less than 10% of the BW effect. Therefore, in principle the muon is a better particle to

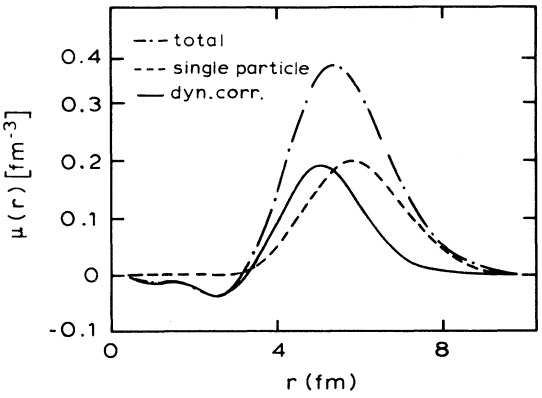

FIG. 1. The normalized magnetization distribution (dot-dashed line) given in terms of the single particle (dashed line) and dynamic-correlation (full line) contributions as a function of the nuclear radius.

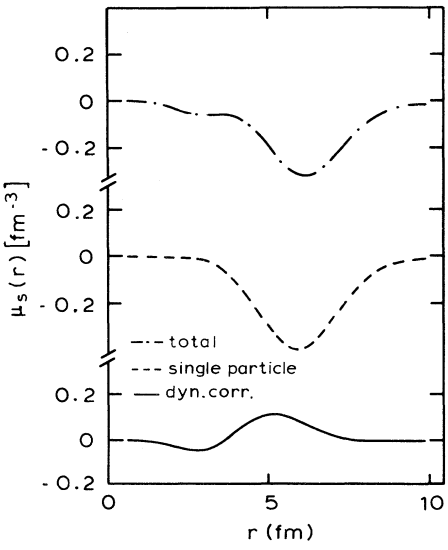

FIG. 3. The spin part of the magnetization distribution given in terms of the single particle and the dynamic-correlation contributions.

test the form of the magnetization distribution. Our calculated value of 4.45 keV of the ground-state HFS splitting in muonic bismuth is in excellent agreement with the experimental result of 4.44 (15) keV [14,15]. Since the calculated size of the BW contribution entering in the splitting is 2.19 keV, this allows a test of our model to a level of 7%, limited unfortunately by the experimental accuracy.

In Fig. 1 we have plotted the normalized total, the single-particle, and the dynamic correlation ground-state magnetization distributions. Figure 2 gives the normalized magnetization distribution due to the angular orbital momentum in terms of the single particle and dynamic-correlation contributions. Figure 3 shows the normalized spin magnetization distribution also in terms of single particle and dynamic-correlation contributions. The spin distribution peaks at a larger radius than the orbital magnetic distribution. This could be associated with the formation of the neutron halo. In Figs. 2 and 3, the normalization factors are different. Figure 4 shows the total ground-state charge distribution in terms of the single particle and the dynamic-correlation contributions.

The calculation of the ground-state charge distribution reproduces the trend already found in Ref. [7].

In conclusion we find that the nonlinear approximation, introduced in this paper reproduces accurately the ground-state properties of the ^{209}Bi nucleus. The

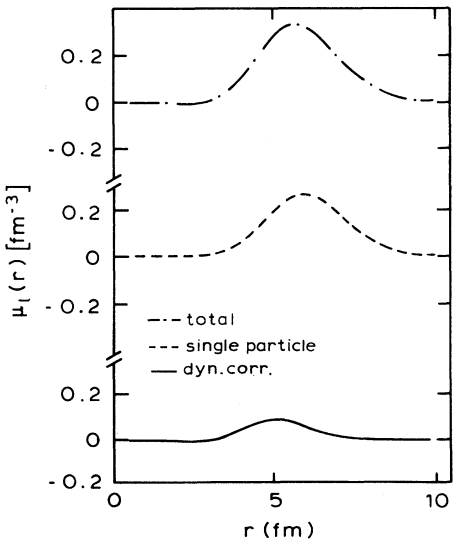

FIG. 2. The angular orbital momentum part of the magnetization distribution given in terms of the single particle and dynamic-correlation contributions.

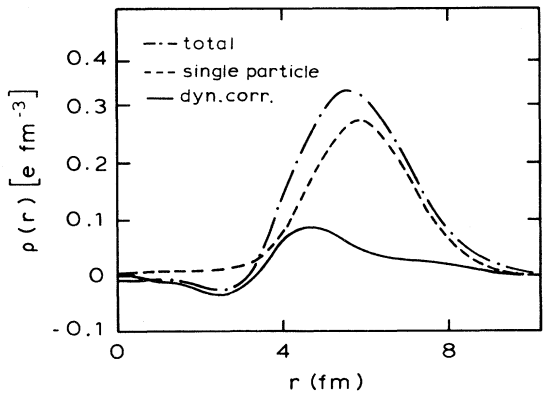

FIG. 4. The normalized charge distribution for the $h_{9/2}$ dynamic-correlated proton given in terms of the single particle and dynamic-correlation contributions.

dynamic-correlation model should therefore be used to calculate the charge-current distributions of nuclei over the whole mass scale in order to test its general applicability.

Our value of 5.091 eV calculated for the HFS splitting of $^{209}Bi^{82+}$ without QED effects is very close to the experimental obtained value of 5.0841 (8) eV. If one combines the results of the calculations of [12,13] with the *BW* effect of this work a value of 5.085 (10) eV is obtained. The indicated uncertainty is obtained comparing calculation and experiment in the muonic case, where the experimental accuracy is the limiting factor. From the calculated vacuum-polarization contribution −0.035 eV [17] we predict a self-energy QED correction of 0.040 (10) eV. A calculation of this contribution is presently under way.

ACKNOWLEDGMENTS

We are very grateful to Professor B. Fricke, Professor W. Greiner, Professor H.-J. Kluge, and Professor G. Soff for fruitful discussions.

[1] H. Noya, A. Arima, and H. Horie, Prog. Part. Nucl. Phys. **1**, 41 (1958).
[2] R. Bauer, J. Speth, V. Klemt, P. Ring, E. Werner, and T. Yamazaki, Nucl. Phys. **A209**, 535 (1973); T. Fujita and A. Arima, *ibid.* **A254**, 513 (1975); C. Mahaux, R. F. Bortignon, R. A. Broglia, and C. H. Dasso, Phys. Rev. **120**, 1 (1985).
[3] I. S. Towner, Prog. Part. Nucl. Phys. **11**, 1991 (1984); T. Ericson and W. Weise, *Pions and Nuclei* (Clarendon, Oxford, 1958).
[4] M. Tomaselli, Phys. Rev. C **37**, 343 (1988); Ann. Phys. (N.Y.) **205**, 362 (1991); Phys. Rev. C **48**, 2290 (1993).
[5] M. Tomaselli, D. Herold, and L. Grünbaum, Nuovo Cimento **46**, 1431 (1978).
[6] M. J. G. Borge, N. Cronberg, M. Cronqvist, H. Gabelmann, P. G. Hansen, L. Johannsen, B. Janson, S. Mattson, G. Nyman, A. Richter, and M. Tomaselli, Nucl. Phys. **A490**, 887 (1988).
[7] R. W. Hasse, B. L. Friman, and D. Berdichevsky, Phys. Lett. B **181**, 5 (1986); M. M. Sharma, G. A. Lalazissis, and P. Ring, *ibid.* **317**, 9 (1993); N. Tajima, P. Bonche, H. Flocard, P. H. Heenen, and M. S. Weiss, Nucl. Phys. **A551**, 434 (1993).
[8] I. Klaft, S. Borneis, T. Engel, B. Fricke, R. Grieser, G. Huber, T. Kühl, D. Marx, R. Neuman, S. Schröder, P. Seelig, and L. Völker, Phys. Rev. Lett. **73**, 2425 (1994).
[9] A. M. Mårtensson-Pendrill, Phys. Rev. Lett. **74**, 2184 (1995).
[10] Morse and Feshbach, *Methods of Theoretical Physics* (McGraw-Hill, New York, 1953).
[11] G. Racah, CERN Report 61 (1961), p. 8; A. De-Shalit and I. Talmi, *Nuclear Shell Theory* (Academic, New York, 1963).
[12] M. Finkbeiner, B. Fricke, and T. Kühl, Phys. Lett. A **176**, 153 (1993).
[13] S. M. Schneider, J. Schaffner, W. Greiner, and G. Soff, J. Phys. B **26**, L581 (1993).
[14] R. Bauer, J. Speth, V. Klemt, P. Ring, E. Werner, and T. Yamazaki, Nucl. Phys. **A209**, 535 (1973).
[15] A. Rüetschi, L. Schellenberg, T. Q. Phan, G. Piller, L. A. Schaller, and H. Schneuwly, Nucl. Phys. **A422**, 461 (1986).
[16] H. Backe, R. Engfer, E. Kankeleit, R. Link, R. Michaelsen, C. Petitjean, H. Schneuwly, W. V. Schroeder, J. L. Vuilleumier, H. K. Walter, and A. Zehnder, Nucl. Phys. **A234**, 469 (1979).
[17] S. M. Schneider, G. Soff, and W. Greiner, Phys. Rev. A **50**, 118 (1994).
[18] M. Le Bellac, Nucl. Phys. **40**, 645 (1963); A. Bohr and V. F. Weisskopf, Phys. Rev. **77**, 94 (1950).
[19] T. T. S. Kuo and G. H. Herling, Report NRL 2258, Washington, D.C. (1971), and private communication (1979).
[20] V. Gillet, A. M. Green, and E. A. Sanderson, Nucl. Phys. **88**, 321 (1966).
[21] Y. E. Kim and J. O. Rasmussen, Nucl. Phys. **47**, 184 (1963); W. Y. Lee *et al.*, Nucl. Phys. **A181**, 16 (1972).
[22] D. Herold, M. Tomaselli, and L. Grünbaum, Phys. Lett. **49B**, 246 (1974).
[23] M. Tomaselli and D. Herold, Report No. 10 IKDA 1977.
[24] E. W. Otten, in *Nuclear Radii and Moments of Unstable Nuclei*, edited by D. A. Bromley (Plenum, New York, 1988), Vol. 7, p. 515; H. de Vries, C. W. de Jager, and C. de Vriex, At. Data Nucl. Data Tables **36**, 495 (1987).
[25] P. Raghavan, At. Data Nucl. Data Tables **42**, 189 (1989).